修士論文

リンパシンチグラムにおけるセンチネルリンパ節のコンピュータ検出支援システムの開発

Computer-aided Detection Scheme for Sentinel Lymph Nodes on Lymphoscintigram

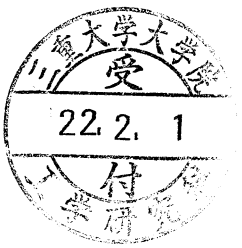

平成 21 年度修了

三重大学大学院 工学研究科

博士前期課程 電気電子工学専攻

川村敏仁

Contents

List of Figures

1. Introduction

1.1. Breast cancer

Breast cancer is one of the major health problems for women health in developed countries. In the United States, one in eight women has breast cancer during their lives [1]. Therefore, it is estimated that about 40,000 women will die of breast cancer in a year. On the other hand, in Japan, MHLW (Ministry of Health, Labor and Welfare) reported that one in twenty women has breast cancer during their lives. Breast cancer has the highest disease rate in all the cancers for Japanese women. In 2007, 11,323 women died of breast cancer [2]. Figure 1 shows the change in the number of women who died of breast cancer in Japan. It is expected that the number of people who die of breast cancer will increase for a while because the disease rate of breast cancer tend to increase. Therefore, the number of breast operative treatments also will continue to increase.

1.2. Sentinel lymph node biopsy

In traditional breast operative treatments, axillary lymph nodes (ALNs) were excised in all patients because it was very difficult to diagnose whether breast cancer had metastasized to the ALNs [3]. The operative treatment for excising the ALNs would compromise the patient's quality of life (QOL), also has the high possibility of giving the patient aftereffects [4-6]. In recent years, sentinel lymph node (SLN) biopsy is becoming popular as an effective method to diagnose whether breast cancer has metastasized to the ALNs. The ALNs diagnosed as negative with the SLN biopsy do not need to be excised from the patients [7]. Therefore, these patients would be able to avoid compromising the QOL.

For the SLN biopsy, the locations of SLNs need to be identified in the patient. RI method [8, 9] is known as one of popular methods for identifying SLNs. This is a method based on characteristic that injected radioactive substance accumulates to the SLNs. Surgeons identify the SLNs by use of a gamma probe and a gamma counter in the beginning of breast operative treatment. However, it takes a long time to identify them because surgeon has to check the gamma counter again and again while moving the gamma probe by little and little. To reduce the identification time, a lymphoscintigram which shows the accumulation degree of the radioactive substance is often taken to know rough location and number of SLNs before breast operative treatment [10, 11].

1.3. Purpose of this study

Although radiologists try detecting the SLNs on lymphoscintigram, it is not easy to detect all of them correctly. This is because not only SLNs but also the neighborhood of injection site appears as areas with high pixel values (gamma count values) on lymphoscintigrams, as shown in Fig.2. Those are the radioactive substance remaining on the injection site and the artifacts (shine-through) caused by the remaining radioactive substance. Therefore, detecting the SLNs in the neighborhood of the injection site mapped on lymphoscintigrams is difficult task because the contrasts between those SLNs and the surrounding background are very low. To reduce the influence of this remaining radioactive substance, radiation from the injection site is shielded sometimes by putting a copper sheet on the site of injection in patient [11]. However, there is a possibility that the copper sheet shields also radiation from the SLNs. Therefore, a novel image processing method for improving the contrast of the SLNs has been desired to detect the SLNs efficiently.

We thought that a concept of computer-aided diagnosis (CAD) schemes [12, 13] for detecting potential regions of lesions in medical images would be able to be applied for detection aid of the SLNs. The purpose of CAD is to improve the diagnostic accuracy and the consistency of the radiologists' image interpretation by taking into account the detection result outputted by CAD schemes as a second opinion. In previous study, many researchers developed CAD schemes for detecting lesions based on the laterally symmetry of normal tissue such as lung field and breast [14-18]. In these CAD schemes, the normal tissues were removed while improving the contrasts of the lesions by the subtraction between right and left normal tissues. On the other hand, the remaining radioactive substance around the site of injection radiates gamma ray

radially. Therefore, the area of the injection site and the shine-through on lymphoscintigram were also expected to become nearly symmetrical, whereas the SLNs appear as asymmetrical spots in the area. The purpose of this study was to develop a CAD scheme for detecting SLNs on lymphoscintigrams by applying the subtraction technique to the symmetry in the neighborhood of the injection site.

2. Materials

Our database consisted of 78 lymphoscintigrams which were obtained by a single injection with technetium colloid (time: 150-seconds, energy window: 140KeV+60KeV). Informed consent was obtained for the research use of each patient's lymphoscintigrams. The size of lymphoscintigram images were 256 pixels by 256 pixels. Although 121 SLNs were identified from 78 patients by the use of a gamma probe in breast operative treatment, only 86 SLNs in them were confirmed retrospectively on lymphoscintigrams by the consensus of two experienced radiologists who referred to the identification result based on gamma probe. Therefore, the locations of 86 SLNs on lymphoscintigrams were used as "Gold standard" in this study.

3. Methods

Figure 3 shows the schematic diagram of our CAD scheme using a subtraction technique based on the symmetry in the neighborhood of the injection site.

3.1. Expansion of lymphoscintigram

It was difficult to analyze the SLNs in detail because they were small on lymphoscintigrams with low spatial resolution. Therefore, the lymphoscintigram was expanded by using a linear interpolation [19]. Figure 4 shows the illustration of the linear interpolation.

$$\textit{Interpolated pixel value} =$$

$$(1-dy)\times((1-dx)\times C_0 + dx\times C_1) + dy\times((1-dx)\times C_2 + dx\times C_3) \quad (1)$$

Here, C_i was the pixel value on the coordinate i. The size of the expansion image was 512 pixels by 512 pixels. Figure 5 shows an example of the expanded lymphoscintigram.

3.2. Segmentation of injection site

Lymphoscintigram which was a nuclear medicine image included many noises. In this study, therefore, lymphoscintigram was smoothed by using a Gaussian filter [19] in order to reduce the influence of noises. The filter size and the standard deviation for the Gaussian filter were given as 11 pixels and 1.2 by taking into account the mean of the size of the SLNs on lymphoscintigrams.

The pixel values in the injection site are very high on lymphoscintigrams. We employed a gray-level thresholding technique [19] to segment the injection site. There is also a pixel with the highest pixel value in the neighborhood of the center of the injection site. The pixel values become much lower at farther pixels from its center in the injection site. For example, Fig. 6(a) showed the line profile of pixel value on vertical straight line through the center of injection site. Therefore, the areas of regions segmented as the injection site were measured by varying a threshold value from high pixel value to low pixel value in the gray-level thresholding technique. Fig. 6(b) showed that the relationship between the gray-level threshold value and the area of segmented region. We consider that the threshold value t into which the area of segmentation region gently changes was the pixel value of injection site. Therefore, the injection site was segmented by using the minimum threshold value t which met conditions of expression (2).

$$f(t) - f(t+5) \leq 20 \tag{2}$$

Here, $f(t)$ was the area of the segmented region with the threshold value t. Figure 7 shows an example of the segmented image for the injection site.

3.3. Subtraction image based on symmetry

To obtain the subtraction image based on the symmetry in the neighborhood of the injection site, the original lymphoscintigram was divided into four regions by the vertical straight line and the horizontal straight line through the center of the segmented injection site, as shown in Fig. 8.

Although the neighborhood of the injection site on lymphoscintigram was expected to become nearly symmetric, it did not completely become symmetric. Therefore, we first defined one of the four divided regions as a target region. We then calculated the correlation coefficients based on the pixel values between the target region and each of the other three regions. The region with the highest correlation coefficient in the other three regions was selected as the similar region for the target region. Figure 9 shows the illustration of the selection of similar region. The subtraction image for the target region was obtained by subtracting the values of pixels in similar region from the values of the corresponding pixels in the target region. Here, the region of interest (ROI) with the size of 3 pixels by 3 pixels was defined at the each pixel in the similar region. The most similar pixel value in the ROI was subtracted from the value of the corresponding pixel in the target region. This procedure was repeated until every region had been used for target region. Figure 10 shows the subtraction image between each of four regions and the similar regions. Here, the pixel values less than zero in the subtraction image were given as zero.

3.4. Enhancement of sentinel lymph nodes

It was necessary to enhance the SLNs in the subtraction images because the contrasts between those SLNs and surrounding background had been relatively low. We defined two ROIs at each pixel in the subtraction image, as shown in Fig.11. The SLNs were then enhanced by the following equation.

$$Enhanced\ image(x,y) = Subtraction\ image(x,y) \times \left(1 - \frac{mean\ pixel\ value\ in\ ROI_2}{mean\ pixel\ value\ in\ ROI_1}\right) \quad (3)$$

The size of ROI_1 was 11 pixels by 11 pixels, whereas that of ROI_2 was 15 pixels by 15 pixels. Here, the pixel values less than zero in the enhanced image were given as zero because the mean pixel value for the ROI_2 should be higher than that for the ROI_1 in the nodular structure such as the SLNs. Figure 12 shows the enhanced image for the SLNs.

3.5. Detection of sentinel lymph nodes

The SLNs had high pixel values on the enhanced image. Therefore, the candidates for the SLNs were segmented by applying a gray-level thresholding technique. However, not only SLNs but also noises were segmented as candidates for SLNs. Size of SLNs tended to be larger than that of noises. Shape of SLNs also tended to be circular. Therefore, we removed the candidates with the area less than 20 pixels or the degree of circularity [19] less than 0.6 as false positives from the segmented image. Figure 13 shows an example of the detected image for the SLNs. When the center of the candidates for SLNs was within a true SLN region determined by two experienced radiologists, this candidate was considered to have been "truly" detected. When the center of the candidates for SLNs was not within a true SLN region, this candidate was considered as a false-positive.

4. Results and Discussion

Figure 14 shows the FROC (Free-response receiver operating characteristic) curve [20], i.e., the relationship between true-positive (TP) fraction and the number of false-positives (FPs) per image, when the threshold value was varied in the segmentation of the candidates for SLNs. The density distribution for the neighborhood of the injection site is expected to be almost constant in lymphoscintigrams obtained under the same conditions. Therefore, we considered that the subtraction image would be also obtained by subtracting the values of pixels in the phantom image for the injection site from the values of the corresponding pixels in original lymphoscintigram for patient. In order to investigate the usefulness of the subtraction technique based on similar regions, therefore, the FROC curve for the computerized scheme based on the phantom image is also shown in Fig.14. Here, the used phantom image was taken under the same conditions when the lymphoscintigram for patient was taken in clinical application. We also used the same criterion of threshold values regarding the pixel value, the size, and the degree of circularity in both our CAD scheme and the computerized scheme using the phantom image. The detection performance of our CAD scheme with the similar regions was much higher than that of the computerized scheme with the phantom image for the injection site. Although we expected that the density distribution on the injection site in lymphoscintigram was comparable to that in the phantom image, those density distributions were large different. It was very difficult to normalize those density distributions on the mapped injection site which had very large variation in the pixel values by simple image normalization such as a linear grayscale transform. Therefore, there were many false positives on the injection site in the detected images obtained by

the computerized scheme with the phantom image. On the other hand, it was not necessary to perform the image normalization because two regions in the same image were compared in our CAD scheme. Therefore, we considered that the number of the false positives was small on the injection site.

Many researchers have developed computerized schemes for detecting lesions based on the laterally symmetry of normal tissue. In order to investigate the usefulness of dividing into four regions, therefore, we attempted to detect SLNs by a computerized scheme with dividing into two regions. In this scheme, the lymphoscintigram was divided laterally into two regions by the vertical straight line through the center of the segmented injection site. The areas with high pixel values in the subtraction image between right and left regions were detected as SLN by use of the same criterion of threshold values concerning the pixel value, the size, and the degree of circularity. Figure 15 shows the FROC curves by our CAD scheme and the computerized scheme with dividing into two regions. The detection performance of our CAD scheme with dividing into four regions was much higher than that of the computerized scheme with dividing two regions. This result would indicate the influence of the not completely symmetric injection site was decreased by using the similar region.

If the sensitivity of our CAD scheme is 100%, surgeons will need only to check the locations detected by our CAD scheme in breast operative treatment. This would improve not only the radiologists' detection performance but also the time for breast operative treatment. The reduction of the operation time leads to the improvement of the patients' QOL. Therefore, high sensitivity was important even if the number of FPs was rather large. With our CAD scheme, the highest sensitivity and the number of FPs were 95.3% (82/86) and 2.51 per image, respectively. Some of the undetected

SLNs exist on the dividing line between regions. The SLN was divided to some regions by the dividing line. The segmented region corresponding to the SLN was then removed as false positives by the criteria for the area. Therefore, it might be possible to improve the sensitivity by changing the criterion for the removal of false positives near the dividing line.

One hundred twenty one SLNs were identified from 78 patients by the use of a gamma probe in breast operative treatment. However, only 86 SLNs were confirmed retrospectively on the lymphoscintigrams by the consensus of two experienced radiologists and were used as "Gold standard" in this study. Therefore, some true SLNs might be included in the false positives.

5. Conclusion

In this paper, we developed a CAD scheme for detection of the SLNs by using a subtraction technique based on the symmetry of the injection site mapped on lymphoscintigrams. With our CAD scheme, the sensitivity and the number of FPs were 95.3% (82/86) and 2.51 per image, respectively. Radiologists would be able to detect the SLNs efficiently on lymphoscintigrams by taking into account the detection results of this CAD scheme as a second opinion.

Acknowledgment

I'm grateful to Prof. Shinji Tsuruoka, Associate Prof. Haruhiko Takase, and Assistant Prof. Hiroharu Kawanaka for useful advice and to Assistant Prof. Ryohei Nakayama at Mie University School of Medicine for teaching and discussions. Many thanks are due to the members of Information Processing Laboratory in School of Engineering, Mie University.

References

[1] American Cancer Society, "Cancer Facts and Figures 2009", 2009

[2] Ministry of Health, Labor and Welfare, "Population Survey Report" (in Japanese), 2007

[3] Fisher B, Bauer M, Wickerham DL, et al : Relation of number of positive axillary nodes to the prognosis of patients with primary breast cancer. An NSABP update. Cancer 1983, Vol.52, pp1551-1557.

[4] Lin PP, Allison DC, Wainstock J, et al : Impact of axillary lymph node dissection on the therapy of breast cancer patients. J Clin Oncol 1993, Vol.11, pp1536-1544.

[5] Ivens D, Hoe AL, Podd TJ, et al : Assessment of morbidity from complete axillary dissection. Br J Cancer 1992, Vol.66, pp136-138.

[6] Recht A, Houlihan MJ : Axillary lymph nodes and breast cancer : a review. Cancer 1995, Vol.76, pp1491-1512.

[7] Krag D, Weaver D, Ashikaga T, et al : The sentinel lymph node in breast cancer – a multicenter validation study. N Eng J Med 1998, Vol.339, pp941-946.

[8] Krag DN, Weaver DL, Alex C, et al: Surgical resection and radio-localization of the sentinel lymph node in breast cancer using a gamma probe. Surg Oncol 1993, Vol.2, pp335-340.

[9] Eshima D, Fauconnier T, Eshima L, et al: Radiopharmaceuticals for lymphoscintigraphy : including dosimetry and radiation consideration. Semin Nucl Med 200, Vol.30, pp25 - 32.

[10] Mc Master s KM, Wong SL, Chao C, et al : Defining the optimal syrgeon experience for breast cancer sentinel lymph node biopsy : Amodel for implementation

of new surgical techniques. Ann Surg 2001, Vol.234, pp292-299.

[11] Cantin J, Scarch H, Levine M, et al : Clinical practice guidelines for the care and treatment of breast cancer ; 13. Sentinel lymph node biopsy. CMAJ 2001, Vol.165, pp166-173.

[12] K. Doi, H. MacMahon, S. Katsuragawa, R. M. Nishikawa, and Y. Jiang : Computer-aided diagnosis in radiology: potential and pitfalls, European Journal of Radiology 1997, Vol.31, No.2, pp.97-109.

[13] R. Nakayama : Toward practical application and spread of CAD for mammography, GE today, GE Healthcare 2007, Vol.23, pp.51-52.

[14] Tsukuda S, Heshiki A, Katsuragawa S, et al : Detection of lung nodules on digital chest radiographs : potential usefulness of a new contralateral subtraction technique. Radiology 2002, Vol.223(1), pp199-203.

[15] Li Q, Katsuragawa S, Doi K : Improved contralateral subtraction images by use of elastic matching technique. Med Phys 2000, Vol.27(8), pp1934-1942.

[16] Li Q, Katsuragawa S, Ishida T, et al : Contralateral subtraction: a novel technique for detection of asymmetric abnormalities on digital chest radiographs. Med Phys 2000, Vol.27(1): pp47-55.

[17] Yin F F, Giger M L, Doi K, Yoshimura H, Xu X W, Balter J, and Meltz CE : Automated registration of digital mammograms for use in mammographic computer vision schemes. Med Phys 1990, Vol.18, pp.524.

[18] Karssemeijer N, and te Brake G M : Combining Single View Features and Asymmetry for Detection of Mass Lesions. Digital mammography Nijmegen 1998, pp.935-1102.

[19] W. Niblack, "An Introduction to Digital Image Processing", Prentice Hall 1985.

[20] Chakraborty D P and Winter L H L : Free-response methodology: alternate analysis and a new observer- performance experiment. Radiology 1990, Vol.174, pp.873-881.

Research Accomplishment

国際会議

[1] Toshihito Kawamura, Ryohei Nakayama, Kan Takeda, Hiroharu Kawanaka, Takahiro Takada, Koji Yamamoto and Shinji Tsuruoka "Development of Computerized Identification Method for Nipple in Mammograms", SCIS&ISIS 2008, pp1847-1852.

[2] Toshihito Kawamura, Ryohei Nakayama, Yosuke Mizutani, Kan Takeda, Hiroharu Kawanaka, Takahiro Takeda, Koji Yamamoto and Tsuuoka Shinji "Computer-aided Diagnosis Scheme for Detection of Mass with Bilateral Subtraction Technique in Mammograms", SCIS&ISIS 2008, pp1853-1858.

[3] Toshihito Kawamura, Ryohei Nakayama, Takanori Ogino, Akiyoshi Hidukuri, Hiroharu Kawanaka and Shinji Tsuruoka "Computerized Extraction Method of Hepatic Vessels in Contrasted Abdominal X-ray CT Images" IWRIS 2009, pp51-54.

[4] Takanori Ogino, Ryohei Nakayama, Toshihito Kawamura, Takahiro Takada, Koji Yamamoto, Naoki Nagasawa and Kan Takeda "Computerized Scheme for Detecting Sentinel Lymph Nodes on Lymhoscintigram using Subtraction Technique based on Symmetry of Mapped Injection Site" SCIS&ISIS 2008, pp1995-1998.

[5] Takanori Ogino, Ryohei Nakayama, Toshihito Kawamura, Akiyoshi Hidukuri and Kan Takeda "Computer-aided Detection Scheme for Sentinel Lymph Modes on Lymposcintigrams" IWRIS 2009, pp43-46.

[6] Akiyoshi Hidukuri, Ryohei Nakayama, Toshihito Kawamura, Takanori Ogino and Shinji Tsuruoka "Computerized Segmentation Method of Calcifications within Clustered Microcalcifications on Mammograms" IWRIS 2009, pp47-50.

国内会議

[1] 川村敏仁，中山良平，荻野隆法，檜作彰良，川中普晴，鶴岡信治，“腹部3次元CT画像における肝臓領域内血管の抽出法”，平成21年度日本生体医工学会東海支部大会，pp24.

[2] 川村敏仁，中山良平，荻野隆法，檜作彰良，川中普晴，鶴岡信治，“差分技術を用いたリンパシンチグラムにおけるセンチネルリンパ節のコンピュータ同定システム”，平成20年三重地区計測制御研究講演会，ppB1-1 － B1-4.

[3] 川村敏仁，中山良平，荻野隆法，檜作彰良，竹田寛，川中普晴，高田考広，山本皓二，鶴岡信治，“乳房X線画像（MLO画像）を対象とした乳頭領域検出法の開発”，第28回医療情報学連合大会，pp1179-1182.

[4] 川村敏仁，中山良平，竹田寛，川中普晴，高田孝広，山本皓二，鶴岡信治，“乳房X線写真における乳頭自動検出法の開発”，第27回医療情報学連合大会，pp.1050-1052.

[5] 川村敏仁，中山良平，竹田寛，川中普晴，高田孝広，山本皓二，鶴岡信治，“乳房X線画像における乳頭領域の検出アルゴリズムの開発”，平成19年三重地区計測自動制御研究講演会，ppA12-1 - A12-6.

[6] 檜作彰良，中山良平，川村敏仁，荻野隆法，川中普晴，鶴岡信治，“対称性に基づいた差分処理によるセンチネルリンパ節の同定法”，平成21年度電気関係学会東海支部連合大会，pp O-203.

[7] 檜作彰良，中山良平，川村敏仁，荻野隆法，川中普晴，鶴岡信治，“形状を維持した個々の石灰化陰影の抽出法”，平成20年三重地区計測制御研究講演会，ppB2-1 － B2-4.

[8] 荻野隆法，中山良平，川村敏仁，檜作彰良，高田考広，山本皓二，竹田寛，“リンパシンチグラムにおける注射部位の対称性に基づくセンチネルリンパ節

の同定法”，平成 20 年三重地区計測制御研究講演会，ppB3-1 － B3-3.

[9] 荻野隆法，中山良平，川村敏仁，檜作彰良，高田考広，竹田寛，山本皓二，“リンパシンチグラムにおけるセンチネルリンパ節部位のコンピュータ同定支援システムの開発”，第 28 回医療情報学連合大会，pp1191-1193.

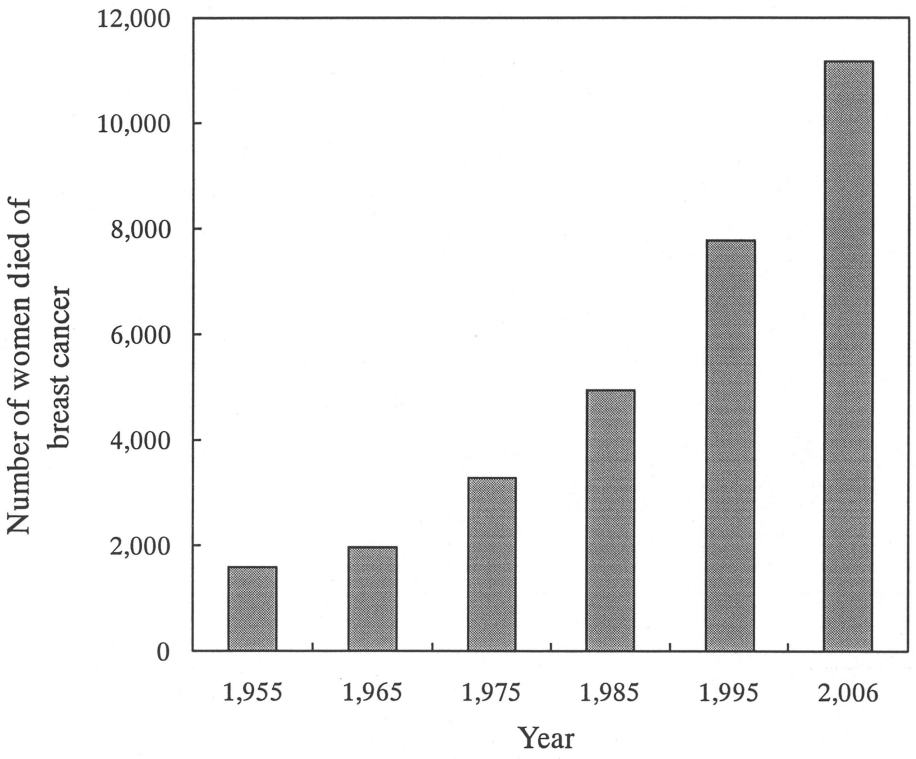

Figure 1 Change in the number of women died of breast cancer in Japan

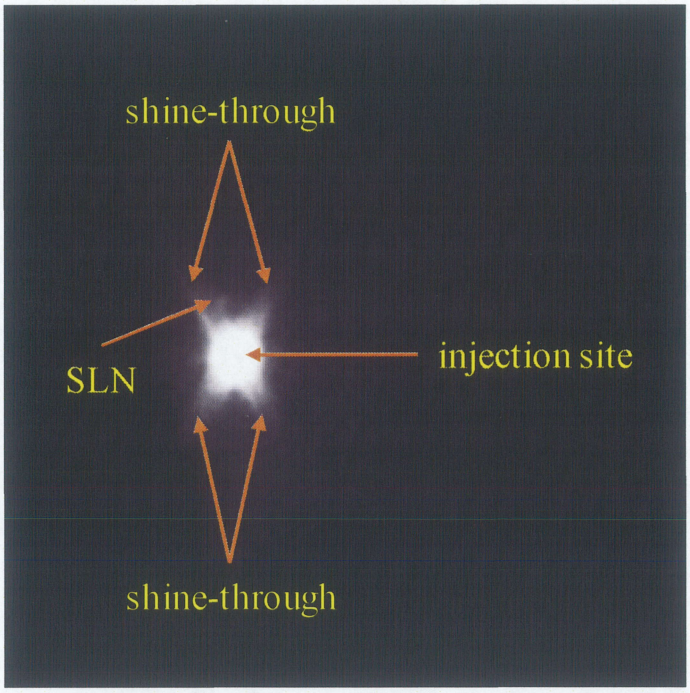

Figure 2　Example of lymphoscintigram

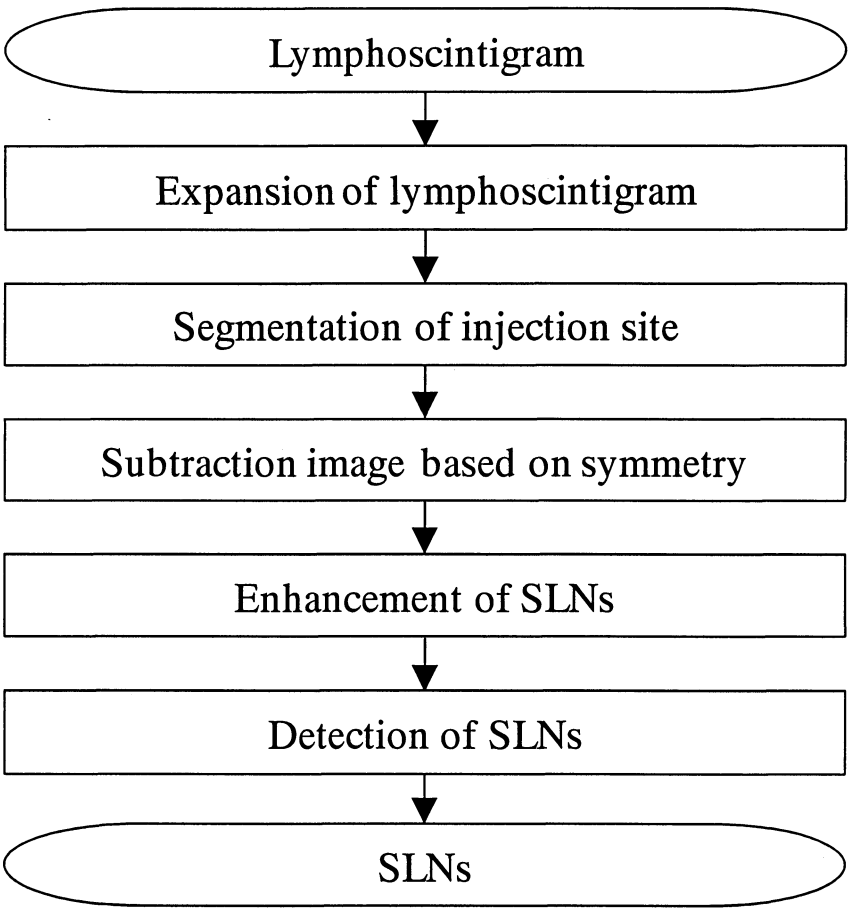

Figure 3 Schematic diagram of our CAD scheme

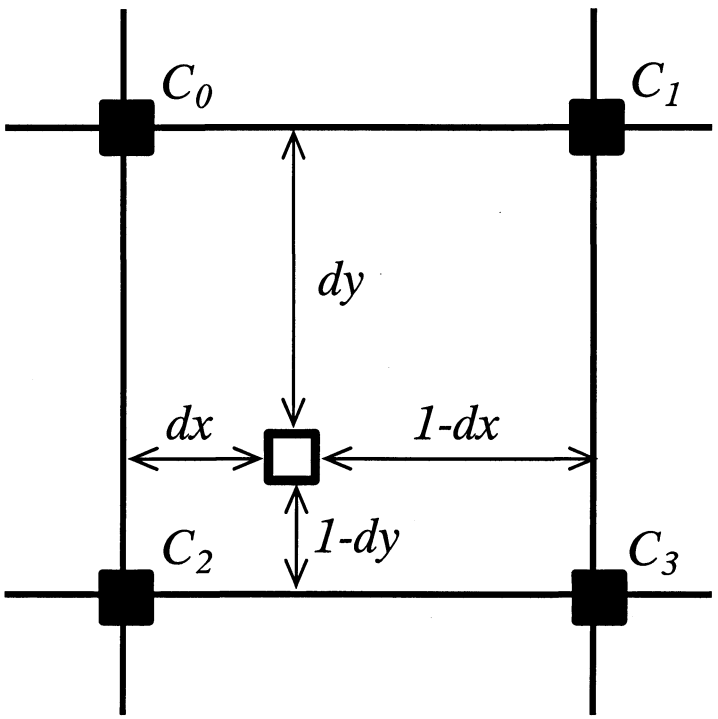

Figure 4　Illustration of the linear interpolation

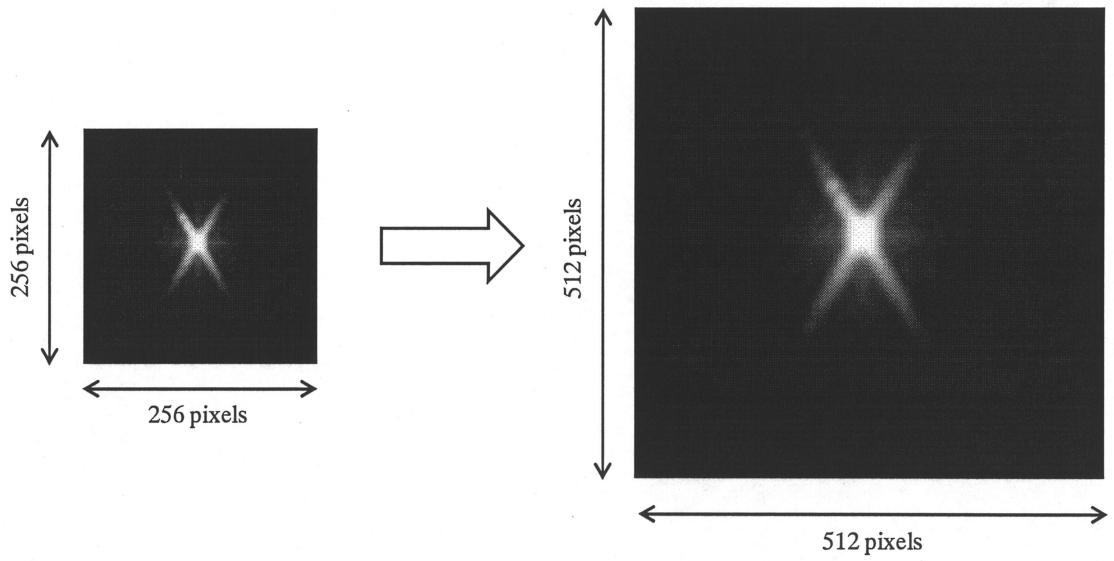

Figure 5 Example of the expanded lymphoscintigram

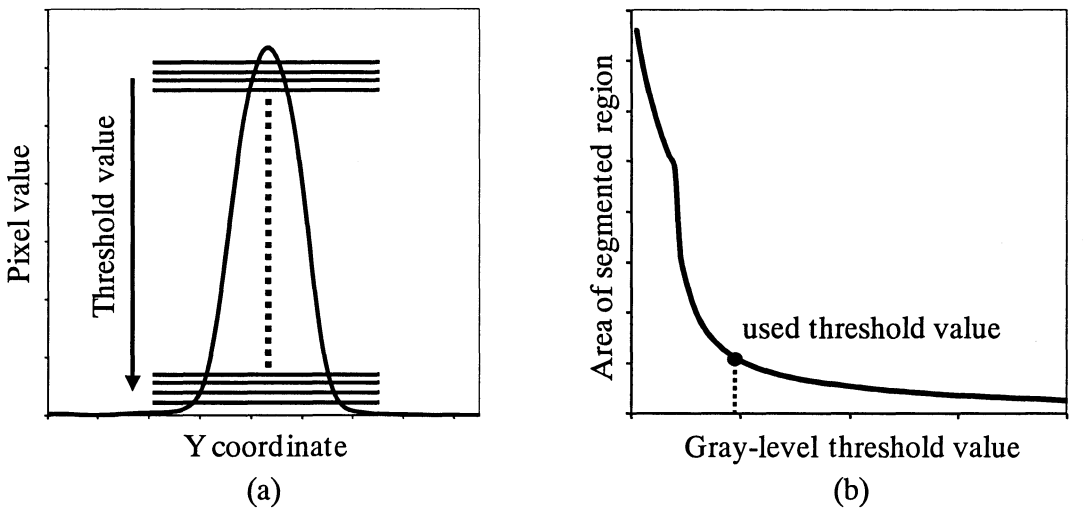

Figure 6 Illustration of segmentation of injection site
(a) Line profile of the y coordinate,
(b) Relationship between the threshold value and the area of segmented region

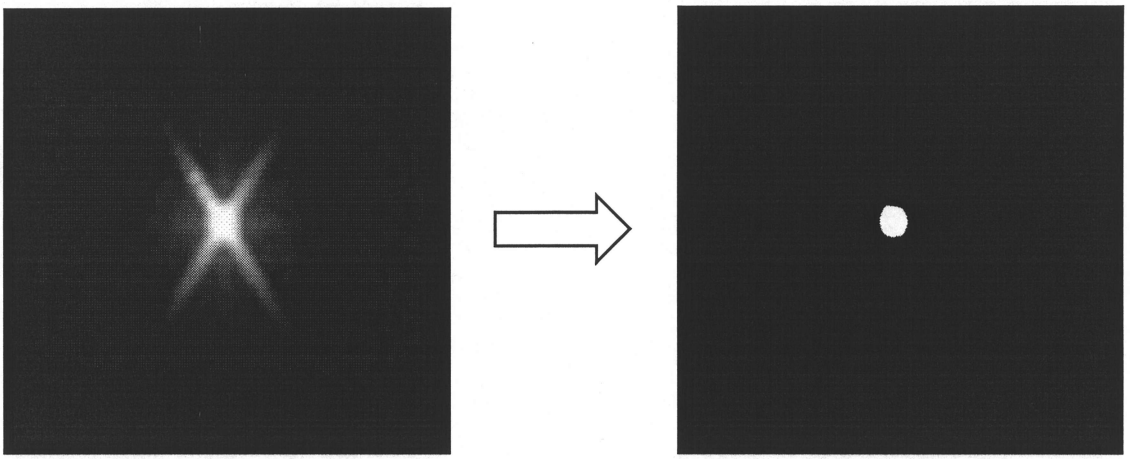

(a) Expanded image　　(b) Segmented image for the injection site

Figure 7　Example of the segmented image for the injection site

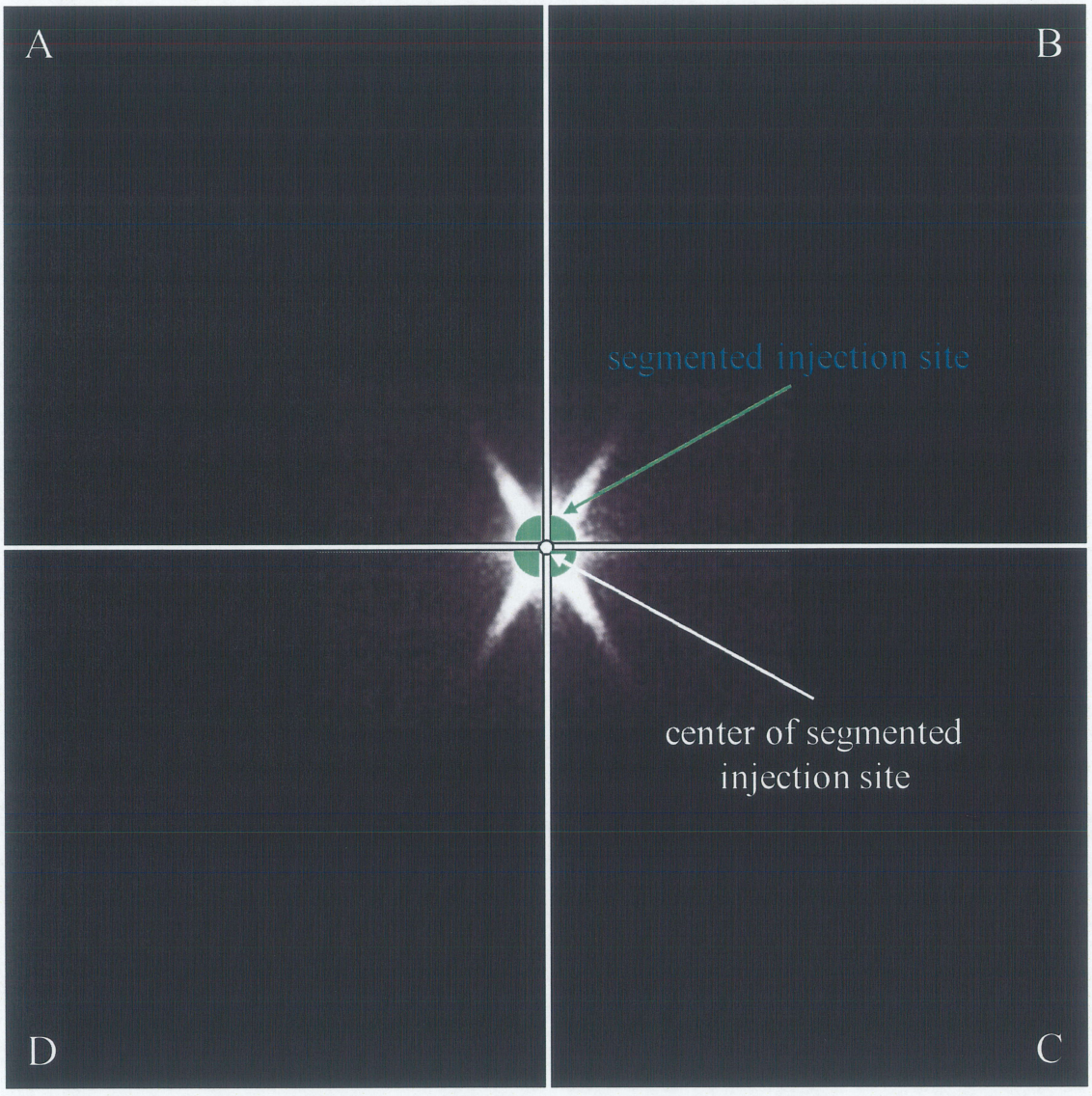

Figure 8 Example of the division of lymphoscintigram

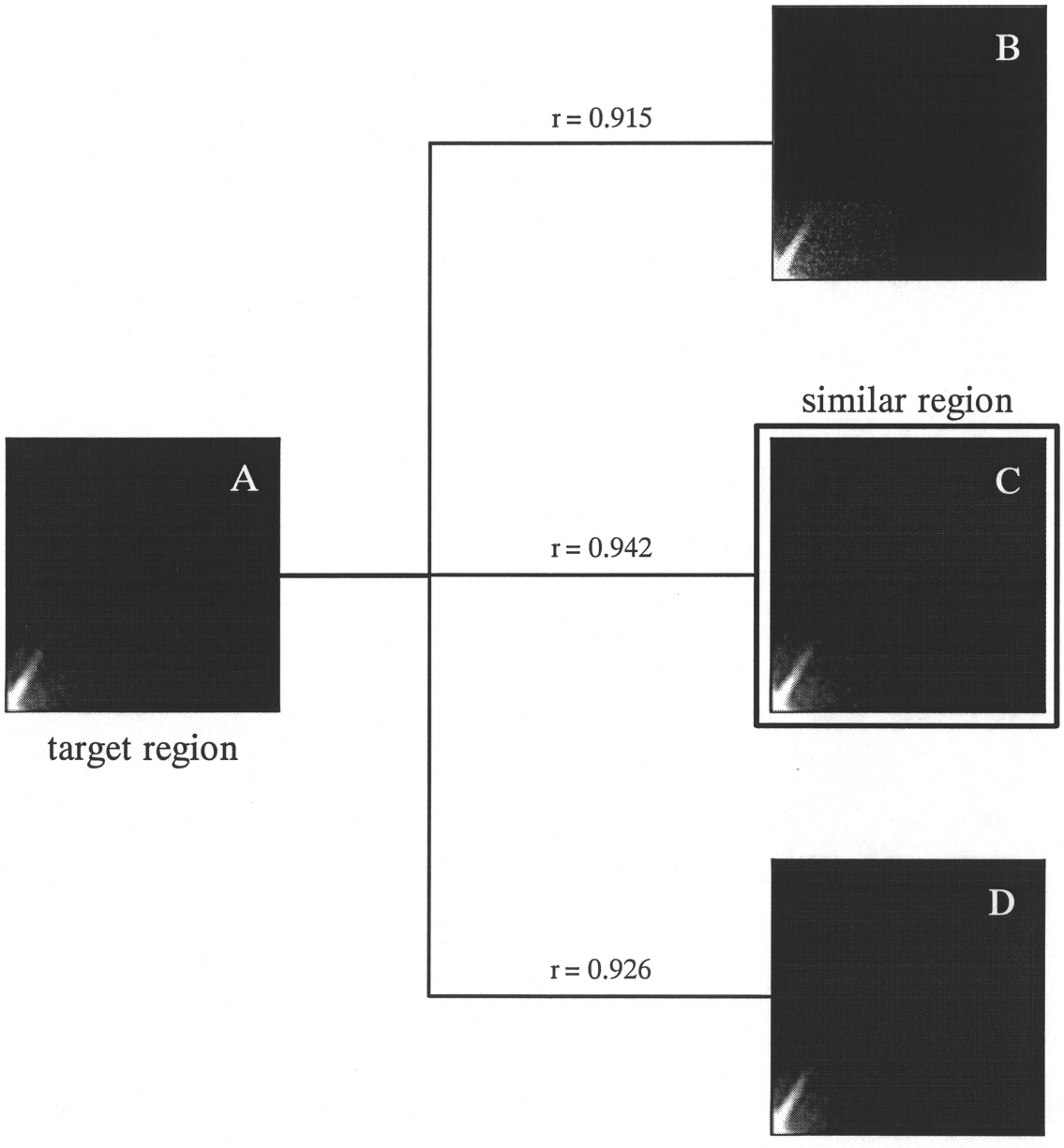

Figure 9 Illustration of the selection of similar region

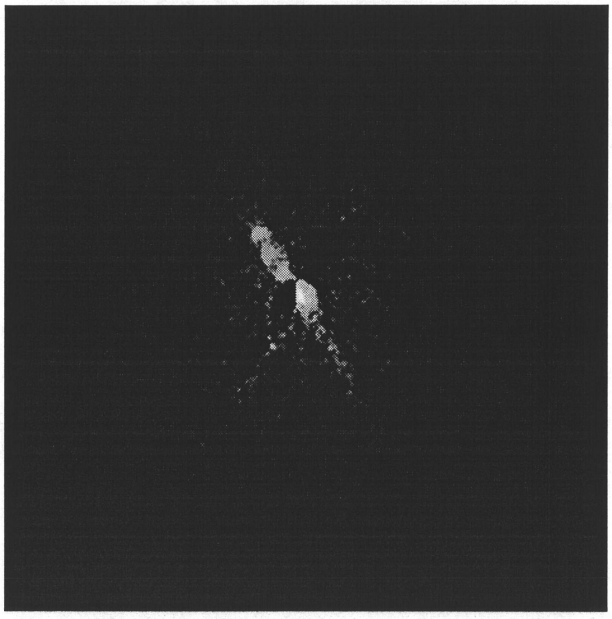

Figure 10 Example of the subtraction image between each of four regions and the similar regions

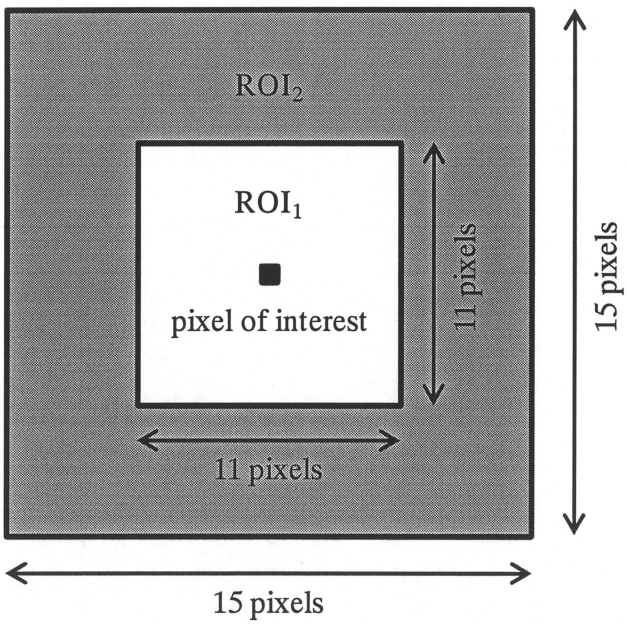

Figure 11　Definition of two ROIs for enhancing the SLNs

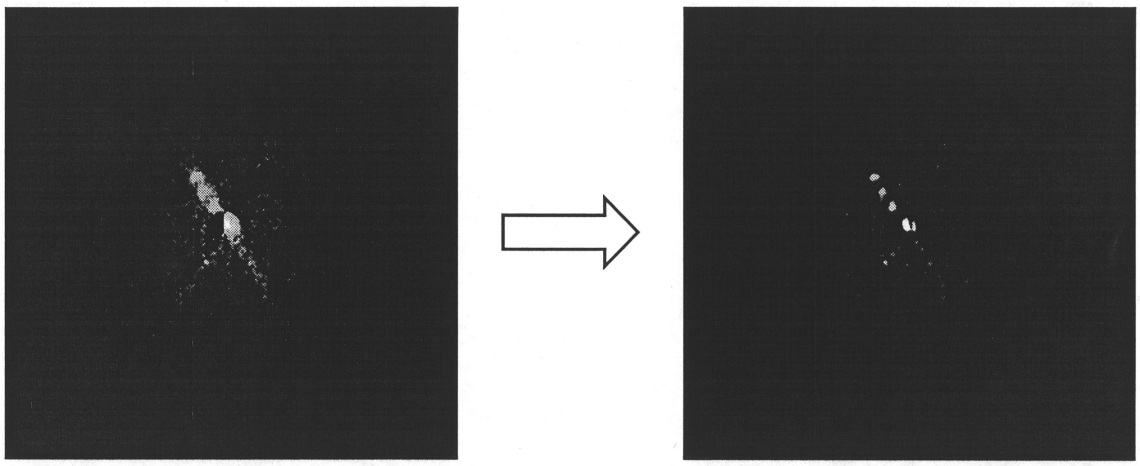

(a) Subtraction image　　(b) Enhanced image for the SLNs

Figure 12　Example of the enhanced SLNs

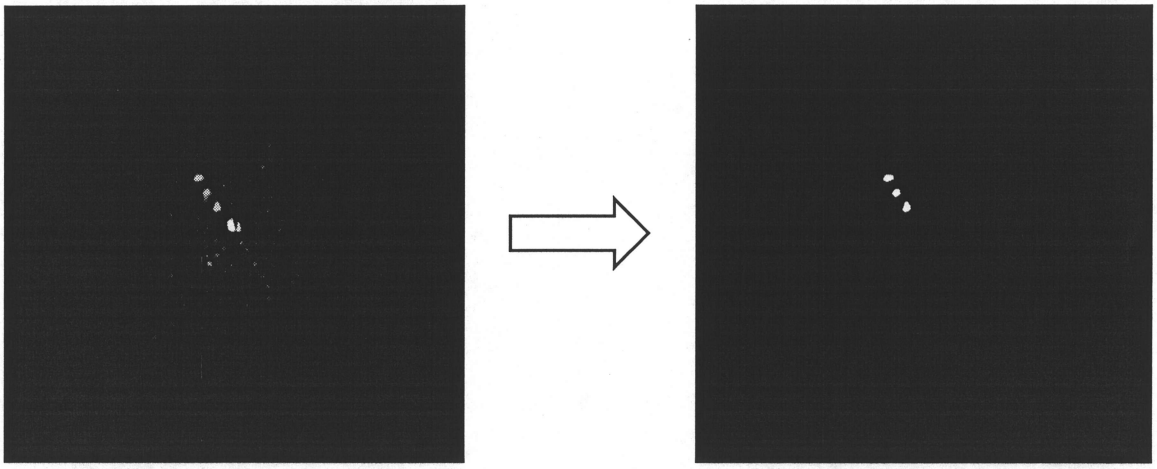

(a) Enhanced image　　(b) Detected image for SLNs

Figure 13　Example of the detected image for the SLNs

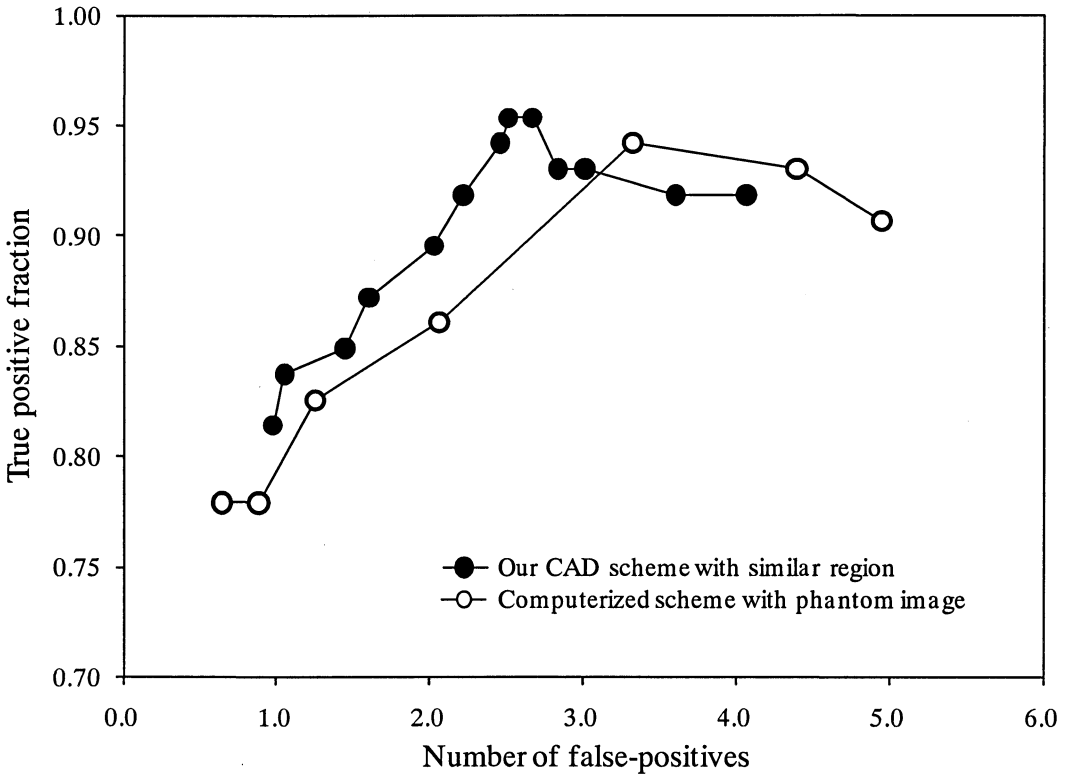

Figure 14 Comparison of between our CAD scheme with similar region and computerized scheme with phantom image in FROC curve

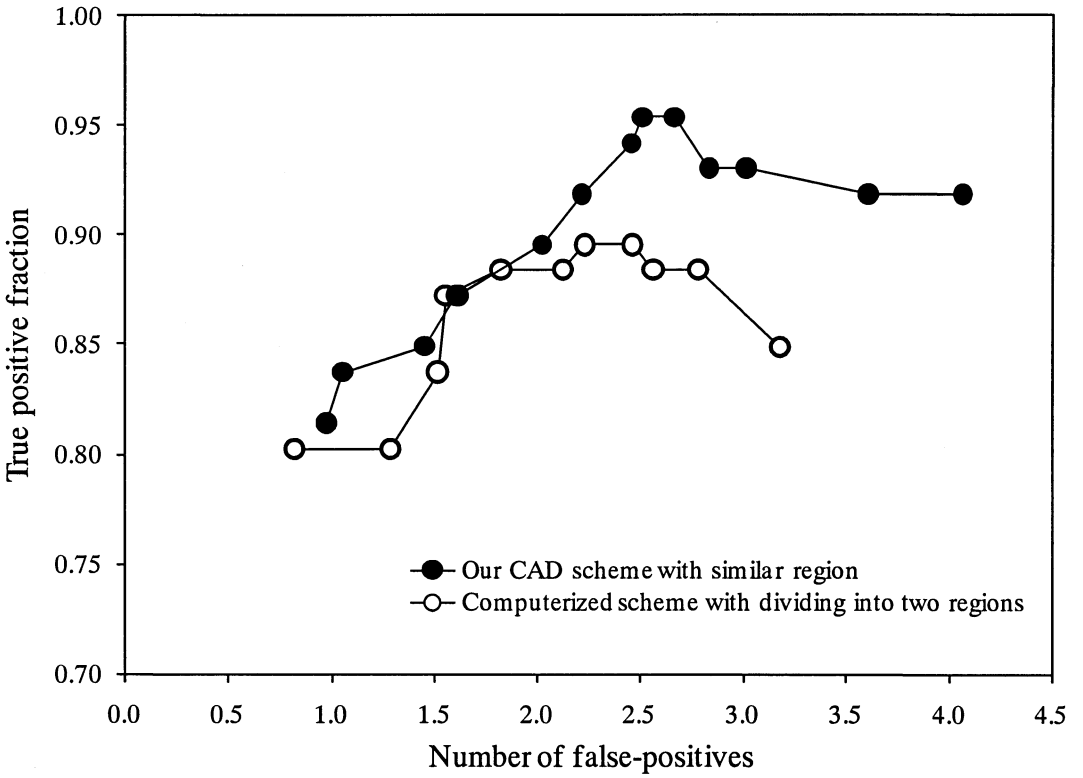

Figure 15 Comparison of between our CAD scheme with similar region and computerized scheme with dividing into two regions in FROC curve